PROCEEDINGS OF SPIE

SPIEDigitalLibrary.org/conference-proceedings-of-spie

Status update of LLAMAS: a wide field-of-view visible passband IFU for the 6.5m Magellan telescopes

Furesz, Gabor, Simcoe, Robert, Egan, Mark, Malonis, Andrew, Masterson, Rebecca, et al.

Gabor Furesz, Robert A. Simcoe, Mark Egan, Andrew Malonis, Rebecca Masterson, Joshua Brown, Gregory Cappiello, Christian Chesbrough, Kristin Clark, David Coppeta, Danielle Frostig, Michelle Gabutti, Samuel Halverson, Erik Hinrichsen, Sabrina Kahn, Madeline M. Lambert, Nathan Lourie, John Piotrowski, Christopher Semisch, "Status update of LLAMAS: a wide field-of-view visible passband IFU for the 6.5m Magellan telescopes," Proc. SPIE 11447, Ground-based and Airborne Instrumentation for Astronomy VIII, 114470A (13 December 2020); doi: 10.1117/12.2562803

SPIE.

Event: SPIE Astronomical Telescopes + Instrumentation, 2020, Online Only

Status update of LLAMAS – a wide field-of-view visible passband IFU for the 6.5m Magellan telescopes

Gabor Furesz[a], Robert A. Simcoe[a,b], Mark Egan[a], Andrew Malonis[a], Rebecca Masterson[a,c], Joshua Brown[d], Gregory Cappiello[d], Christian Chesbrough[d], Kristin Clark[d], David Copetta[d], Danielle Frostig[a,b], Michelle Gabutti[a], Samuel Halverson[a], Erik Hinrichsen[a], Sabrina Kahn[a], Madeline M. Lambert[c], Nathan Lourie[a], John Piotrowski[d], and Christopher Semisch[d]

[a]MIT-Kavli Institute for Astrophysics, 77 Massachusetts Ave., Cambridge, MA, USA
[b]MIT Department of Physics, 77 Massachusetts Avenue Cambridge, MA, USA
[c]MIT Department of Aeronautics and Astronautics, 77 Mass. Ave., Cambridge, MA, USA
[d]MIT Lincoln Laboratory, 244 Wood Street, Lexington, MA, USA

ABSTRACT

The Large Lenslet Array Magellan Spectrograph (LLAMAS) is an NSF-funded facility-class Integral Field Unit (IFU) spectrograph under construction for the 6.5-meter Magellan Telescopes. It covers a $37'' \times 37''$ solid angle with 2,400 optical fibers efficiently coupled by a double-sided microlens-array, producing $R = 2,000$ spectra with $0.75''$ spatial resolution. Its broad passband from $\lambda = 350 - 970$nm offers access to line and continuum measurements over a wide range in redshift. Light is multiplexed by the IFU into 8 compact, carbon-fiber bench mounted spectrographs utilizing VPH grisms. We employed several trades on cost-performance ratio while optimizing LLAMAS' system design including: (a) Splitting the passband between 3 fast all-refractive camera systems with modest entrance pupils, (b) limiting the fibers per unit (i.e. slit length) and building more spectrographs to leverage on production volume, and (c) using a commercial CCD camera built around a common detector (e2v 42-40) and thermoelectric + liquid cooling. To boost blue throughput and achieve high-quality sky subtraction the spectrograph cluster is mounted next to the focal plane on a folded Cassegrain port with gravity-invariant support. This also allows the instrument to deploy quickly, and be fully accessible within 10 minutes on any night, serving as a facility unit for observing astrophysical transients. A sub-sized IFU (169 fibers), mounted in a full-sized front end package with a single spectrograph (2 cameras) was delivered to Magellan in March 2020. We present as-measured laboratory performance from this prototype, though on-sky commissioning was unfortunately cancelled because of the COVID-19 pandemic. This contribution therefore focuses on subsequent design evolution and status of the full facility instrument.

Keywords: spectrograph, IFU, fiber feed, lenslet array, fast camera, VPH

1. INTRODUCTION

The Large Lenslet Array Magellan Spectrograph (LLAMAS, see Figure 1) is a new facility instrument designed for the Magellan Telescopes, to obtain (1) rapid and efficient spectroscopy of astrophysical transients discovered by the Large Synoptic Survey Telescope (LSST), (2) single-pointing redshift and dynamical measurements of galaxy clusters identified by Sunyaev-Zeldovich surveys of the Southern sky, and (3) single-pointing emission and absorption measurements of Lyα and metal-enriched gas flows within the circumglactic halos of distant galaxies.

To best serve these science requirements we defined LLAMAS' architecture (see Section 2) as a fiber-based (2,400 element, $0.75''$/spaxel), large field-of-view ($37'' \times 37''$), medium spectral resolution (R$\sim$2,000), visible passband (350-975nm) spectrograph. Funded through the NSF MSIP program, LLAMAS is now under construction at the MIT Kavli Institute for Astrophysics and Space Research. As a facility-class instrument it will be available to all scientists within the Magellan consortium, and also to the entire US community over a 4 year period through the public-access provision of the MSIP program. Expected first light is now mid-2022, which represents

Ground-based and Airborne Instrumentation for Astronomy VIII, edited by Christopher J. Evans, Julia J. Bryant, Kentaro Motohara, Proc. of SPIE Vol. 11447, 114470A · © 2020
SPIE · CCC code: 0277-786X/20/$21 · doi: 10.1117/12.2562803

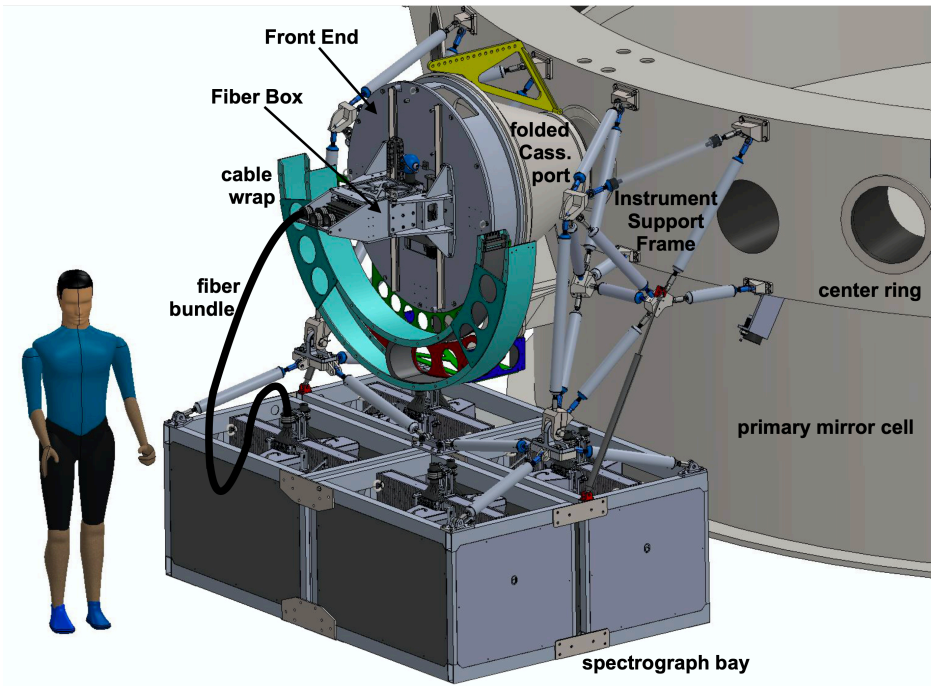

Figure 1.
The LLAMAS instrument on the central folded Cassegrain port of the Magellan telescope center ring. The primary mirror cell outside wall partially visible below the center ring and other ports shown empty for clarity. The LLAMAS Front End and extending Fiber Box is top center, cradled from beneath by the cable wrap of the conical port adapter/instrument rotator. The space frame supports the Spectrograph Bay, consisting of four identical Units, each carrying two spectrographs. For clarity only one fiber cable bundle is shown, feeding one spectrograph.

a delay of approximately six months from the original baseline. This delay is directly traceable to the effects of COVID-19 on global supply chains and local regulations on in-person laboratory integration activities.

LLAMAS will be the first seeing-limited, arcminute-class IFU available on a large US telescope. To place it in context of other facilities Figure 2 summarizes the capabilities of current and future worldwide IFUs, projecting the six-dimensional design space of (1) field of view Ω_{FoV}, (2) spatial resolution Ω_{spaxel}, (3) sky filling factor f, (4) spectral bandpass $\Delta\lambda$, (5) spectral resolution R, and (6) telescope aperture D – all onto a single plane. IFUs at the upper right deliver more information but at higher cost because the CCD pixel count grows volumetrically. Each point's diameter is proportional to its instrumental etendue, $\Omega_{FoV} D^2 f$; the contours represent loci of constant information content (roughly proportional to cost), increasing in factors of ten.

In this paper we will give a high level overview of LLAMAS' system architecture (Section 2) while also providing description of each subsystem. This is followed by some more details of selected design solutions (Section 3). Companion papers in these proceedings (Frostig et al. 11447-118, Furesz et al. 11447-111) detail the optical design and analysis. In Section 4 we discuss some aspects of the design and implementation that could benefit groups contemplating similar instrument designs in the future.

Given the complexity of the instrument and the design approach we have taken—to replicate spectrographs and recycle design elements—we elected to mitigate technical risks by first building a full scale single unit prototype for Magellan's visitor instrument port. Work on this protoLLAMAS instrument commenced in 2017, before the NSF MSIP grant supporting the full instrument build was awarded. While internal resources were limited for this prototyping effort necessitating some simplifications (e.g. 2 spectrograph channels instead of 3) we still designed and built the prototype using final vendors in anticipation of contracts for the full instrument. We

Further author information: send correspondence to G. Furesz at gfuresz@mit.edu

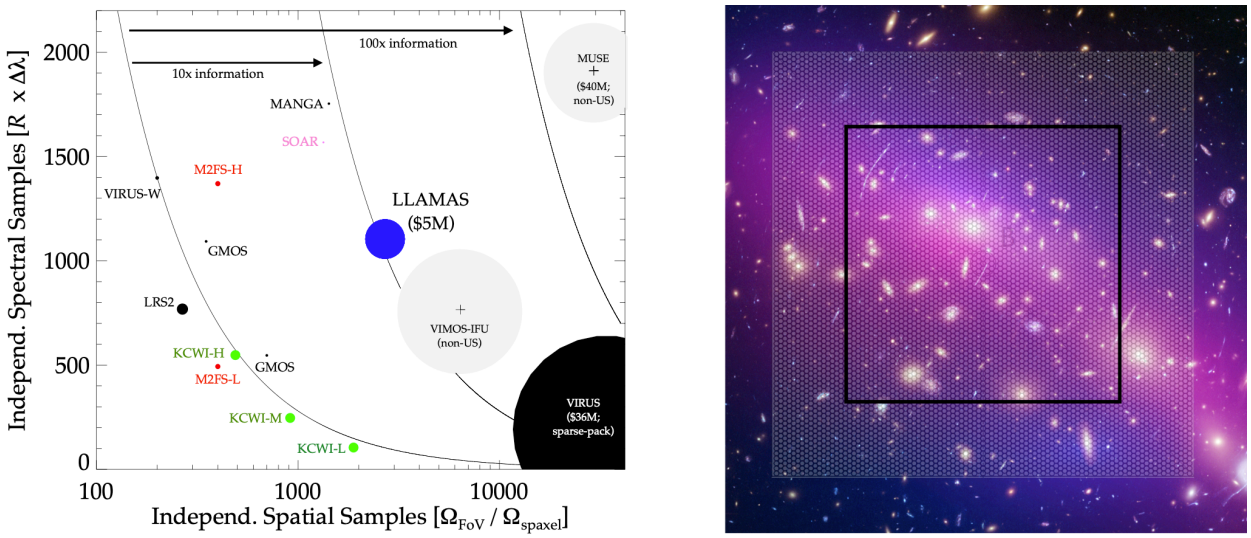

Figure 2.

Left: Information grasp of selected existing or planned IFUs, indicating the number of independent spatial samples and spectral samples. Symbol sizes denote instrumental *etendue* as defined in text with contours of constant information content. While most US facilities cluster along the left contour or have small etendue, LLAMAS will provide the US with a deep, wide-field survey IFU in the Southern hemisphere, competitive with, and in some ways complementary to ESO's MUSE [1] and VIMOS [2] on the VLT. *Right*: HST image of a galaxy cluster with overlay (white grid indicating the sampling) of the LLAMAS micro-lens array pattern. We designed the microlens for $1'\times1'$ FoV, but funding and other limitations resulted in the smaller, $37''\times37''$ actual field that is implemented for LLAMAS (thick black line).

delivered protoLLAMAS to Las Campanas Observatory March 2020, but given the pandemic we were not able to commission it on sky. Nevertheless we document here some lessons learned through the Assembly, Integration and Test (AIT) process that have been folded into the final facility instrument.

2. SYSTEM ARCHITECTURE

Our design flows from Level 1 Science Requirements identified by the three major applications listed in Section 1. Using a simplified version of systems engineering practices developed for MIT's NASA missions, we traced these into Level 2 System Requirements defining the basic instrument parameters such as spectral resolution, sampling pitch, and FoV. These are largely verified by design, but they flow down to detailed Level 3 Technical Requirements that are verified either by design or by explicit performance testing during pre-ship integration. This process is summarized in Figure 3.

A key issue that arose early in the project was the mounting port on the telescope. Time-domain requirements of rapid response and guaranteed availability argue for permanent mounting, which would be only available using one of Magellan's unpopulated bent-Cassegrain ports. Yet instrument size and complexity instead favor installation at Nasmyth platforms, with their gravity invariant location and generous weight/volume allocation. However, 3 of Magellan's 4 Nasmyth foci (on 2 telescopes) have other instruments permanently mounted, and the 4th is a visitor instrument port and therefore has very restricted scheduling. Given the fiber coupling between the spectrographs and the telescope the folded port is actually very viable for the *Front End* of LLAMAS, as the fiber based image slicing, the calibration light injection and an atmospheric dispersion compensator can fit in a relatively small volume. A long *Fiber System* can offload the instrument from the telescope but adversely impacts blue throughput, which is a key competitive advantage for LLAMAS. The solution has been to mount the bank of 4 *Spectrograph Units* (each unit enclosing 2 spectrographs) in the immediate vicinity of the IFU Front End, attaching it to the center ring of the telescope structure via an *Instrument Support Frame*. This solution only uses 5m total length of optical fibers. We addressed the effects of variable gravity-induced flexure

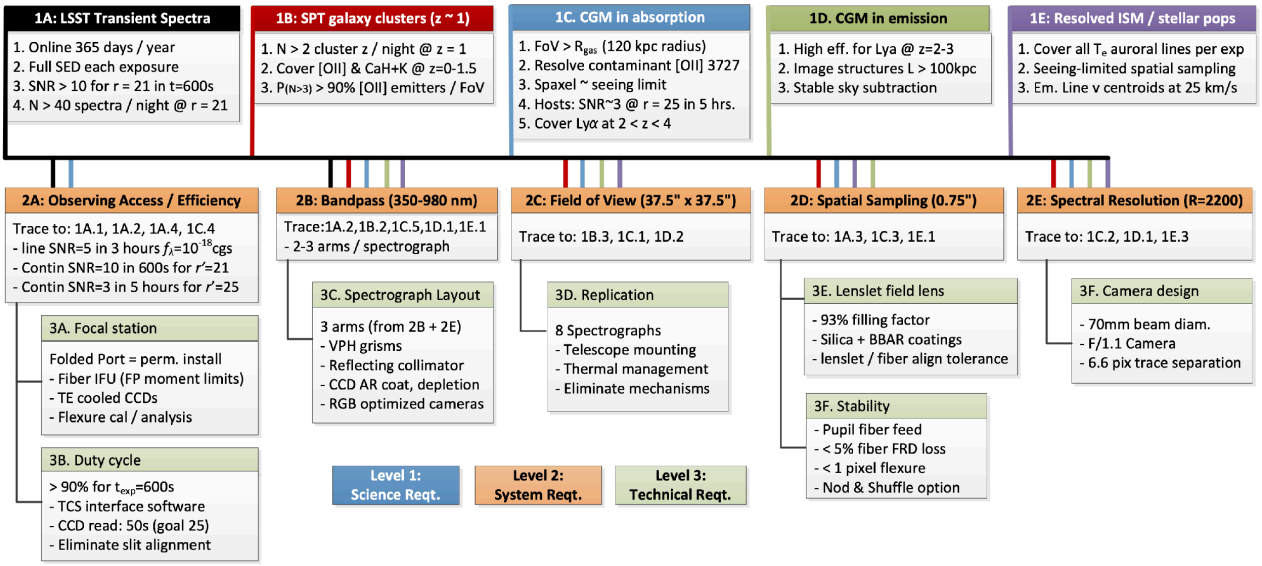

Figure 3.
High-level overview the LLAMAS Science Requirements (top) flowing down into Level 2 System design requirements (orange, middle), which then drive subsystem architectures (green, bottom).

by vertically orienting our four optical benches and loading them symmetrically on either side, while also allowing the spectrographs to pivot as the telescope changes elevation.

The LLAMAS prototype spectrograph was designed for the Magellan II (Clay) Telescope's visitor port, which is a Nasmyth platform with a rotator interface similar to the folded ports. However access is much easier and the spectrograph unit could remain on a cart, supported by the platform, simplifying the prototype design. We still used 5-meter optical fibers, and although only one side of the carbon fiber optical bench was populated with optics, the enclosing Spectrograph took up a volume comparable to one unit cell of the full instrument. The prototype bench is also oriented vertically within the frame, with counterweights simulating the balanced gravity load. The handling cart design allowed rotation to mimic elevation change of the telescope. We used this feature in the lab to evaluate the need/benefit of pivoting the spectrograph bays of the full instrument.

2.1 Front End

The Front End is built on a round baseplate which mates with the instrument rotator of the telescope port. To meet stiffness requirements while keeping the weight and manufacturing costs low (e.g. stock 7075 aluminum plate) we employ two steel T-bars bolted to the interface plate. Between these a stepper driven ball screw drives a linear stage, supported by a follower rail along the opposing edge. This platform serves dual purposes and accordingly has two defined positions: it carries an atmospheric dispersion compensator (ADC) assembly on one end and the calibration system assembly on the other. The ADC is designed around two counter-rotating zero deviation prisms that carry no net optical power, thus do no alter the telescope's native f/11 focal ratio. The calibration unit consists of an integrating sphere with a selection of arc lamps (Kr, Ne, Ar) directly attached to the sphere for wavelength calibration. An Energetiq laser driven light source (LDLS) provides flat field illumination, fiber coupled to the integrating sphere. Light emerging from the sphere is collected by a Fresnel lens and refocused by another one, mimicking the telescope's focal ratio as it illuminates the fiber based image slicer. A fold mirror was necessary to project the calibration light into the IFU as back focal distance of the port is limited. Most components of the calibration system are visible on the left panel of Figure 4.

The Front End's other major subassembly is a fiber box, consisting of several subsystems. Light entering from the telescope through the ADC (or from the calibration system) first meets a bi-stable iris shutter, then the focal plane mask plate. This linear stage allows a closed position for mechanical protection of the microlens array

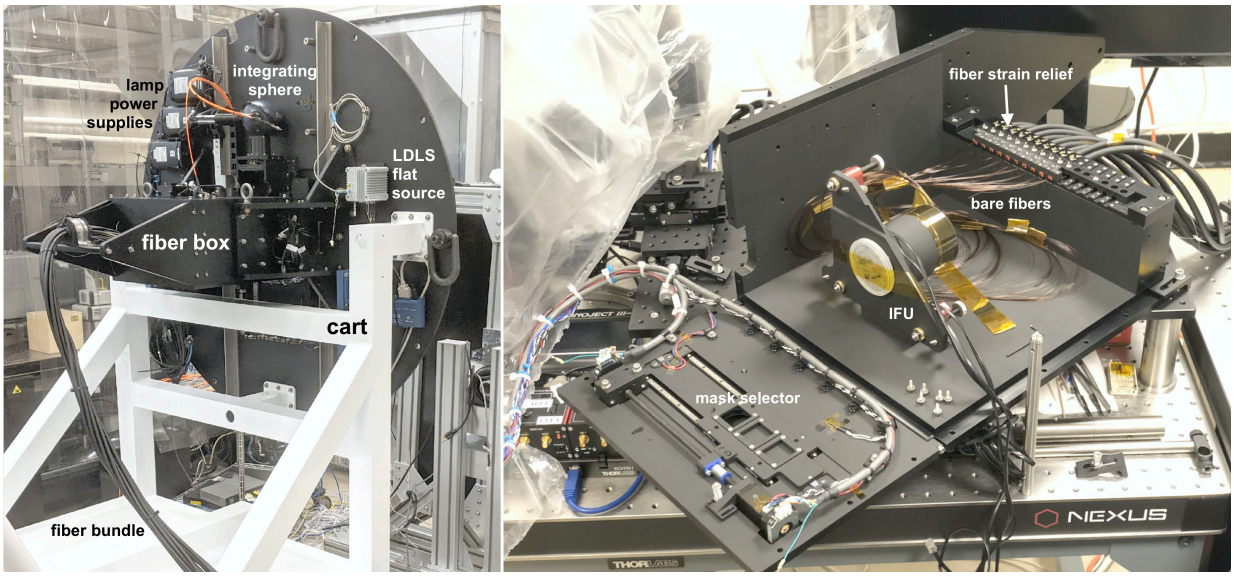

Figure 4.
Left: The protoLLAMAS Front End, which is nearly identical to the full instrument Front End, on its handling cart. Calibration system components are visible on the upper half of the round telescope interface plate, from which the fiber box protrudes perpendicularly to the left. *Right*: The fiber box open during integration, showing the individual fiber bundle strain relieves (upper right), the bare fibers that the box protects as those run to the IFU unit. This is enclosed in the triangular part with a cylinder attached to it, shown in the middle, with the MLA protected by a cover. The folded down front plate contains the mask selector (no masks installed, just empty frames). The volume of the fiber box was designed to accommodate all 2,400 fibers, while in the prototype (shown here) we only deployed 169.

(the front element of the IFU), a fully open position that allows illumination of the entire IFU, and two masked positions for exposing two complementary populations of the fibers. More on this is given in the accompanying optics paper.

The Integral Field Unit is situated just 0.5mm behind the focal plane mask plate, so the focal plane masks are in near-focus. The IFU consists of a double sided microlens array (MLA), closely coupled to a fiber plug plate (FPP). The bare fibers exit this sandwich within a cylindrical tube that offers protection and immediate strain relief. This sleeve and the MLA+FPP assembly are supported by a triangular plate that needs to be precisely aligned to the mask plate as well as to the chief ray of the telescope. To aid this the plate is kinematically mounted to the front of the fiber box and the three fine threaded support legs are adjustable via remote controlled piezo drives, allowing for gap adjustment and tip-tilt control. More on the optical design and performance of the fiber based IFU, the MLA and FPP can be found in the accompanying paper describing the optical and fiber system (see Furesz et al. 11447-111, these proceedings).

2.2 Fiber System

The main design driver for the fiber box is to protect and accommodate the routing and handling of bare fibers during the delicate assembly of the IFU. During integration (see right panel of Figure 4) the fiber box is open and secured to a custom-designed fiber bonding station. The MLA-FPP assembly can be removed and flipped for inspection of the front side. The fiber plugging of cleaved bare fibers happens from the backside of the FPP, and once the array is completed the MLA gets added to the front side of the FPP after cleaning and inspection of the fiber ends.

The light guides are Polymicro FBPI 110μm core step index all fused silica fibers. For the prototype we used 110/132/140 core/clad/buffer fibers, stripped the polyimide buffer using a 3SAE FPU II unit and terminated them through the cladding using a Vytran LDC-200 cleaver. However, the stripping was time consuming and

the plasma torch process compromised the mechanical strength of the fibers—a major problem for AR coating, handling and bonding. Also, the relatively thin cladding is less ideal for cleaving, so for the full instrument we opted for a 110/154/170 dimension fiber (1.4 clad/core ratio) of the same type. Similarly to DESI we also decided to cleave through the buffer directly. The alignment between the FPP and MLA is automatically set by mating micro-machined, matching features during assembly. These are cut into both parts allowing for $<5\mu m$ lateral and axial registration between the two, set by the accuracy of the photo-litographic and photo-assisted etching processes used in the manufacturing of the MLA and FPP. For more details see Furesz et al. 11447-111 in these proceedings.

The bare fibers are bundled in groups of 20, out of which we only count 15 fibers to be used. The large fraction of spares (25%) was determined from our own experience of handling and AR coating the fibers, the desire to only bond in ones with both ends fully intact, as well as advice from the DESI team (Jerry Edelstein, private communication).

After leaving the IFU unit, the fibers run bare for about 0.75m in short coils with the aid of removable shelves that keep rows of outgoing fiber bundles separate. The output end of the fiber box contains 8 rows of strain relief strips, each able to hold 20 PVC coated stainless steel braided hoses (SAWSPP-5N, made by Hagitech in Japan, imported by Jalux Americas). The bare fibers are clamped by RTV pads at the hose entrance, and enter the tubes through 3D printed, rounded plastic orifice inserts to protect them from sharp edges of the terminated hose. Each spectrograph unit receives 20 of these 3.5m fiber tubes with 20 fibers – but as mentioned only 300 of the 400 incoming fibers are bonded into the spectrograph slit. The overall instrument consists of $8 \times 20 = 160$ fiber hoses, or 3,200 optical fibers in total, out of which 2,400 are active. In comparison the prototype uses 10 fiber tubes and contains 200 fibers in total, out of which 169 are active.

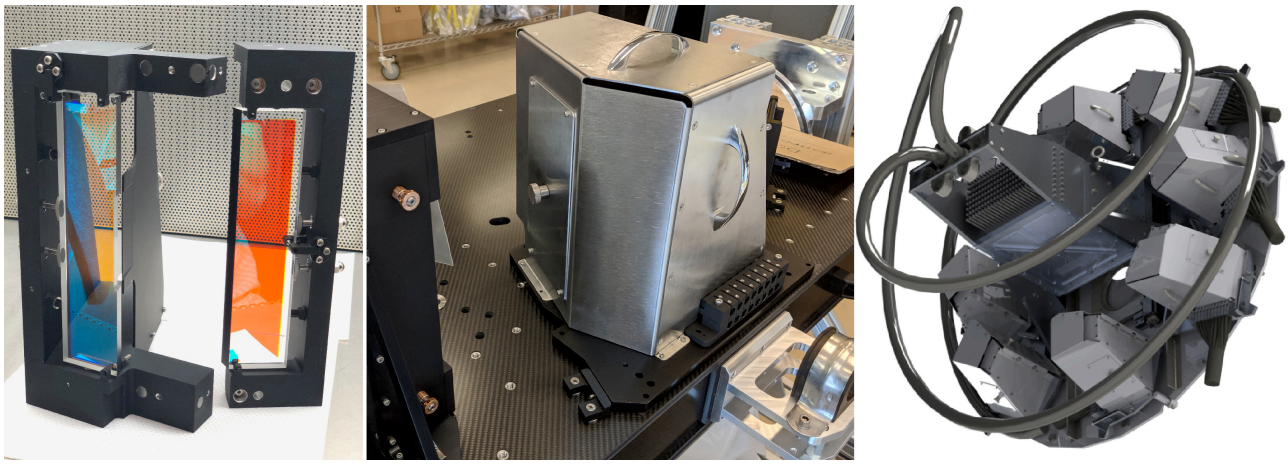

Figure 5.
Left: The two dichroic halves mounted in their respective frames. The stationary base frame (left) holds the slit plate and contains the fiber blade, which provides strain relief and ensures a thin profile for the fiber bundle as it comes off of the slit plate. (The slit plate is not mounted yet, only its bond-pocket is visible). The smaller frame (right) is kinematically mounted and fully adjustable. It is attached after the fibers are all conveniently populated and then it is aligned to the stationary half using an interferometer. *Middle:* The dichroic subassembly shown with the unpainted steel cover, placed on the CFRP optical bench (no fibers installed). The collimator is visible on the left. Facing it is a removable door of the cover, cut to the size of the clear aperture. The cover offers mechanical protection as well as light baffling. *Right:* CAD model showing how the final Front End and telescope interface plate will be carrying the 8 dichroic assemblies, and thus the full fiber assembly, for shipping. This allows the overall LLAMAS instrument to be broken down to five larger components (Front End and Fiber System, and four Spectrograph Units),simplifying handling and shipping.

All fibers were cut to the same length (within $\sim$ 1mm) before inserting them into the protective, watertight but flexible tubes that offer a minimum bending radius of 80mm. Before inserting the bundle of 20 fibers into the tubes we coiled them up and inserted them into custom fixtures used in deposition of anti-reflection (AR)

coatings. This had to be done with the bare fibers as outgasing, volume and handling constraints did not allow for AR coating after insertion of the fibers into the protective hoses. Each such fixture was 0.2×0.2×0.2m in size, contained 5 fiber bundles and uniformly exposed the 5×20×2=200 fiber ends at the center of one facet of the fixture. (See see Furesz et al. 11447-111 in these proceedings for more details.) Cascade Optical could mount 8 such fixtures into their coating chamber of at once, so it took 4 rounds of reloading these eight units to get all fibers coated.

The same strain relief design is used on the spectrograph end as it is in the fiber box. As a secondary measure we also clamped the overall bundle of the braided hoses right after the Front End fiber box and at the entrance of each Spectrograph Unit, reinforcing the strain relief for each individual steel tube. At the spectrograph all fibers are anchored to the dichroic baseplate, and the entire dichroic subassembly can be pulled from the instrument. This allows for building, handling and shipping the Fiber System independently of the Front End or the Spectrographs. The dichroic baseplate is kinematically mounted to the optical bench, allowing for easy and precise reassembly. It also carries a very sturdy, steel cover that doubles as baffle once its protective covers are removed, exposing the clear aperture. Replicas of the kinematic receiver base are temporarily mounted to outer perimeter of the Front End base plate for shipping, with the fiber cables wrapped around the central Fiber Box. This allows for a very compact and secure transportation of the Fiber System, and lets us handle the 4 Spectrograph Units completely independently. More details on the dichroic are given in Section 3.3. Also see Figure 5 and Furesz et al. 11447-111 in these proceedings.

2.3 Instrument Support Frame

As mentioned in the Introduction one of the biggest design challenges was to accommodate the large and complex LLAMAS instrument on the Magellan telescope in a way that (a) keeps the fibers under 5m in length (b) uses one of the folded Cassegrain ports and (c) provides a benign flexure environment for the spectrographs. The observatory also requires unhindered access to other folded port focal stations. Finally, mechanical clearances for telescope maintenance—especially the removal of the primary mirror cell for re-aluminization—had to be accommodated.

As shown in Figure 6 we developed an articulating pivot design for the support frame, which maintains a constant gravity vector while staying within the balancing capability of the telescope. To simplify the design we requested access to the center folded port (currently occupied by the FIRE IR spectrograph), as this location allows for a more compact, symmetric frame design with much simpler implementation of the pivoting spectrograph bays. Currently the 3rd port is undeveloped, but the observatory is building the conical shaped instrument adapter with the associated de-rotator and guider assemblies.

Pivoting instruments do affect telescope balance once they reach hard stops at their travel limits. We aimed to keep the center of gravity (CG) of LLAMAS as close to the telescope as possible , in order to minimize the moment arm associated with telescope balance. Consistent with science requirements, the instrument rotates freely up to telescope zenith angles of 60 degrees (airmass 2.0). However telescope maintenance sometimes requires horizon pointing, at which point the CG of LLAMAS will move, requiring careful accounting in the telescope control system.

2.4 Spectrograph Unit

Operational constraints dictated by the observatory necessitated a very compact packaging of the spectrographs, with additional motivation coming from the relatively small floor- and clean room space available to our group for onsite AIT. The pivoting frame approach simplifies opto-mechanical designs, allowing for smaller, lighter components. To further reduce the overall volume, saving some additional weight and cost, we drew from heritage of the conceptual design for the WISDOM spectrograph [3], where we symmetrically loaded a vertically oriented carbon fiber bench. For LLAMAS the mirrored symmetry is exact, therefore the load path remains in the face-sheets of the bench, which is optimal. To avoid any stress imposed by the bench support we use a 2-point mount. One is fixed in location but allows 3-axis rotation (ball joint) while the other constrains motion in two directions allowing for slip and rotation in the third (axle pre-loaded into a V seat). Given there is no moment due to full symmetry, low clearance hard stops can prevent any unwanted, accidental rotation within

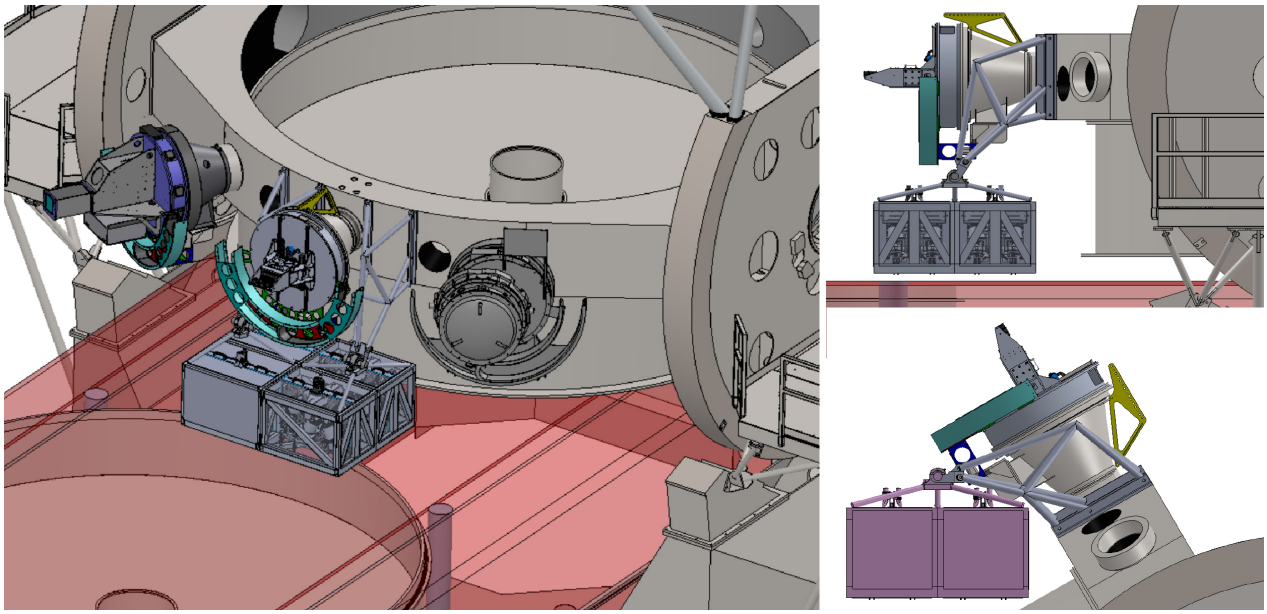

Figure 6.
Left: LLAMAS shown on the destined center folded port of the Baade telescope's center ring, with two other already existing instruments shown (FIRE and MAGE, currently in different arrangement). It was an important guideline in the design of the frame, supporting the pivoting spectrograph bay under the front end, to leave sufficient access to the other instruments, the primary mirror cell and especially for its removal (depicted in transparent red here). *Right panels* show the conceptual clearances for zenith (top) and 30° elevation (airmass=2, bottom) pointing.

a support frame, even if the frame is flexing under external stress. This way no deformations are enforced onto the bench itself.

This approach allows for a simple, rectangular, welded aluminum frame to support one bench carrying two spectrographs (see Fig 7). The open frame with the vertical bench provides good access to all components, and light-tight side panels can be constructed with simple geometry to seal and protect the sensitive spectrograph components. The four detachable frame quadrants are equipped with casters, allowing pairs of spectrographs to be easily moved around in our constrained lab environment during AIT and temporary storage as we go through the sequential build of units. More importantly this simplifies navigation of doors and hallways, as well as the use of a modest service elevator, since our lab is on the 5th floor of an older building not constructed with development of large instruments in mind. The concept of a "Spectrograph Unit" is beneficial for shipping as well, keeping the individual containers manageable in size. This enables air transport from the U.S to Chile, which is our preferred method given the more controlled environment and better oversight compared to sea shipment.

The Unit frames are open on one side, allowing the insertion of the bench to the frame and providing better access for removing/installing the dichroic assemblies. During observatory integration each spectrograph unit is checked out individually, and then the frames simply bolt together forming the overall Spectrograph Bay structure. This attaches to the telescope-mounted support frame via two tripods with turnbuckle adjustable legs. These enable leveling and matching the set (and by its nature, less controllable) spacing of the attachment points provided by the telescope frame (See Fig. 1 and 6).

The right panel of 7 shows a cleaner, closer view of the very compact spectrograph assembly. The short/long pass dichroic (split at 690nm) with the embedded fiber slit is front and center, with the incoming fibers clamped to its base. To the left is the tall, spherical collimator mirror with its support buttresses. In A second blue/green dichroic (split at 475nm), is visible behind the semi-transparent beam. The beam opens up towards the collimator as the fibers are fanned out at the slit to satisfy the Schmidt condition. More on the dichroic mounts can be

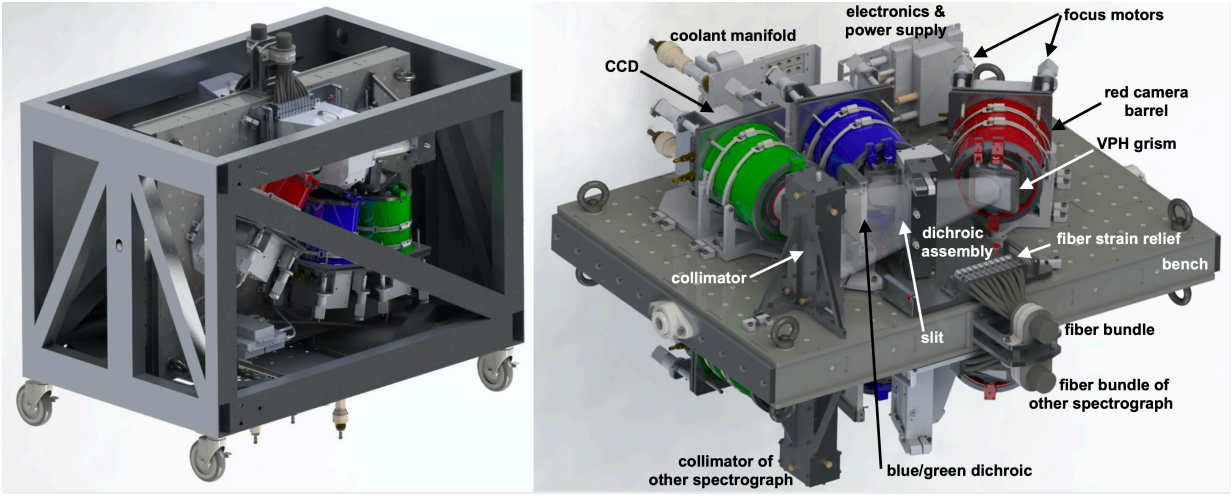

Figure 7.
Left: A single Spectrograph Unit, the rectangular frame with the vertical optical bench inside, carrying two spectrograph assemblies. *Right:* a close up and direct view of the assembled, very compact spectrograph. The optical layout, for comparison/reference, can be found in the accompanying paper describing the optical design of LLAMAS. Seen behind the optics are housekeeping components: power supply, control electronics and coolant distribution manifolds.

found in Sec. 3.3.

Each camera barrel carries the VPH grism assembly in the front, supported by a fully adjustable frame. Rotation of the grisms (to align the orientation of the dispersion axis) is enabled by a slip-ring base on the front of the camera barrel. Tilt, to allow for centering the beam on the camera optics, is achieved by a pair of flex-pivots and a spring loaded 100 TPI adjuster pushing the grism mount. The VPH gratings are implemented in-between a pair of 5mm thick fused silica plates with the prism directly bonded onto the front plate. The whole grism is secured into an aluminum mount using a 5mm thick silicone bond (RTV 60) that covers the entire side of the VPH sandwich (10mm tall bond line). A 3D printed baffle can be attached to the rear of the grism mounting frame, which is the closest location to the pupil.

The camera barrels sit in lightweight double V cradles, preloaded and secured by straps. The entire camera assembly (detector, camera lens and VPH grism) can be adjusted together by moving the base of this kinematically supported subassembly. The initial location is determined by a precision cylindrical insert of the CFRP bench receiving a tooling ball on the bottom of the baseplate. This is our general mounting scheme, allowing for easy assembly and simple collimation of the optics. More on this is given in Sec 3.2. Fine tuning the position and adjusting tip-tilt is achieved by push-pull actuator/lock-screw pairs against steel pads (also built into the bench for the perpendicular preloads) or hard stop blocks (which attach to threaded inserts of the bench).

While the prototype uses the same optical design and opto-mechanical implementation as the production units, protoLLAMAS employs a slightly longer focal length (90mm vs 70mm). This is because early concepts of the instrument aimed at lower spectral resolution ($R \sim 1,300$ vs 2,000) and used only two optical arms instead of three to cover the same passband (350-975nm). This meant using larger detector pixels (e2v CCD 55-30, 22.5μm) with slight undersampling of the PSF. We started building the prototype based on this earlier concept, and some long lead items got locked in (e.g. the CCD, camera optics) while the instrument evolved based on the feedback we received during early proposal reviews. Ultimately we built the prototype to accommodate every aspect of the final concept (e.g. dichroic and collimator large enough to accept full slit of 300 fibers, contracted the same vendors who would – and could – deliver the production units, prescribed the same size optical bench with both sides developed with inserts, etc.). But we had already been locked in for the detector and 2-arm design for protoLLAMAS. Still, it allowed us to fully validate every subsystem and design element, qualify vendors and AIT processes.

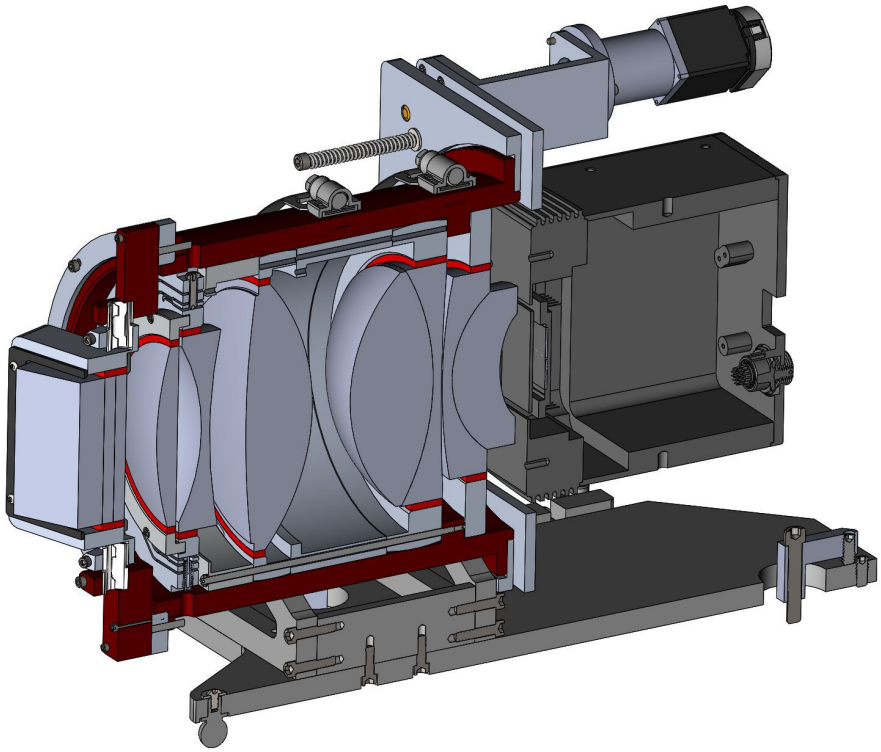

Figure 8.
Cross sectional view of the LLAMAS spectrograph camera assembly. Left is the VPH grism, placed at the minimum overall beam size which is at the center of curvature of the collimator. This is also the pupil of the camera optics. The larger elements in the middle of the optical train are necessary to accommodate the external pupil location while also allowing for the large FoV dictated by the detector. The commercial Raptor Photonics CCD camera is on the right, without showing proprietary inner details.

Attached to the back of the camera lens barrels are the commercial CCD detector heads, built by Raptor Photonics around the venerable e2v CCD 42-40 architecture ($2k \times 2k$, $13.5\mu m$pixels). The compact heads ($126 \times 126 \times 124$mm) offer a lifetime vacuum sealed enclosure for the sensor with a sapphire window and 6.5mm back focal distance, which was a key factor for successful optical design of the fast (effective f/1.05, in polychromatic light and across all field positions) camera optics. The incorporated 5-stage thermoelectric cooling with a liquid heat exchanger offers a $\Delta T > 110°$C with the hot side at 20°C. Thus by running a chilled coolant at 10°Cwe can reach a sensor temperature where dark current is below our target of 0.001 $e^-\ pixel^{-1}\ sec^{-1}$. This is set so the read out noise (RON) would still exceed drk current, and sky noise would exceed total detector noise for a long (> 900 s) science exposures, even at 350 nm.

A stringent requirement for low-systematic sky subtraction has driven the design to accommodate nod & shuffle operation. As it requires bi-directional parallel clocking of the detectors we had to procure a custom sensor build that supports non-inverted mode operation (NIMO) for the 42-20 devices. For the red channel (690-975nm) we opted for deep depletion to suppress fringing and achieve higher efficiency. Given the increased silicon volume requested grade 0 for cosmetics while for the blue (350-475nm) and green (475-690) arms we prescribed grade 1 units. The first two of the 27 production cameras we have received so far from Raptor Photonics achieve $2.3e^-$ read noise at 75kHz readout rate, an excellent performance which is critical for the science operations. (Note: Raptor also achieved excellent RON performance – under $3.0e^-$ – with the prototype NIMO deep depletion CCD 55-30 devices at 75kHz, while implementing the same camera features.)

2.5 Control System

LLAMAS has relatively few user-configurable mechanisms and therefore only requires simple custom solutions for instrument control. However the system required a high degree of replication (24 cameras to focus, each using 3 motors – see Sec 4) so we decided to build the control system electronics based on a Raspberry Pi 4 Model B+, augmented with Arduino MEGA 2560 and custom connector boards. These are cheap, widely available and general platforms so supplying spares with the instrument delivery and throughout its operation cost effective and supply is not a problem. However, this is also not a system specifically designed for precision motion control, so additional effort was needed to develop custom routines and low level software.

The control system and software suite are designed to be net-based, scripted and expandable. All image acquisition, housekeeping, and mechanical actuation is triggered via TCP/IP, minimizing the amount of wiring that has to be run from the control system to the instrument and eliminating the need for interface-specific hardware expansions on the control computer. With the exception of the camera server daemon and associated operations all console operations, data logging, housekeeping queries and hardware actuations are designed to operate using Python for easy portability and reconfiguration. The developed, LLAMAS-specific custom Python library enables easy implementation of high level GUIs, loggers, and control scripts.

The camera server daemon handles all communication with the custom Raptor cameras using an integrated Pleora Cameralink/GigE converter to enable net-based communications and data acquisition. Communication with the server daemon also takes place over a TCP/IP socket. The console makes use of Python dictionaries to format human-readable commands into Raptor serial command syntax and transmit it to the server daemon. The console is also the program which coordinates communication with all of the other system components other than the Raptor Photonics cameras. This includes the Raspberry Pis which are used for triggering, actuation, and housekeeping, as well as communication with the observatory's Telescope Control System. The console also formats received image buffers into FITS format and compiles headers with relevant observation data.

A more substantial effort is required to supply the observer with useful feedback on data quality and reduce spectral data to science-quality products. For quality assurance we provide a quick-look tool for observers to generate spectral images based on archival flat fields and wavelength solutions, and extract spectra of single fibers for offline analysis. Because we developed and integrated model of the instrument that yields fully simulated 2D spectra we can develop pipeline software before the start of the AIT phase.

2.6 Support and Handling Equipment, Observatory Infrastructure

As described above the design of LLAMAS incorporates some handling fixtures into the instrument itself. However, the integration of spectrograph subassemblies onto the optical bench and the optical alignment process requires full access and horizontal positioning of the optical table. Therefore we have built a cart using extruded 80/20 T-slot aluminum components and COTS hardware which orients the bench horizontally with either side facing up, and positions it vertically to transplant the finished spectrograph into the unit frame using a small hoist. (See left panel of Fig 9) For protoLLAMAS this cart was built somewhat larger so it could carry and allow pivoting of the whole, full-size Spectrograph Unit frame. This allowed us to experimentally determine flexure in the lab, mimicking different telescope elevations and see on the images how a fixed (non-pivoting) attachment of LLAMAS to Magellan would affect performance. This led to the strong preference towards the pivoting instrument support frame, with support of the observatory management.

The choice of TE cooling of the camera heads was made to simplify daily operations. However, it requires a significant heat dissipation capacity via circulation of chilled (10°C) liquid coolant. The overall LLAMAS instrument generates 3.5kW waste heat, which must be carried away and discharged outside of the dome. LLAMAS has a complex distribution manifold, flow meters and emergency shutoff valves for each bench. This, along with the circulation manifolds inside the 24 camera heads, generates significant resistance against the flow of the coolant. Between the final heat dump location (down wind, at the end of a tunnel under the telescopes) and the instrument there is a large distance and elevation change as any piping needs to go through the telescope cable de-rotator and climb up the telescope pier and mount. This further increases the requirements for the pump system which needs to provide adequate flow rate (1.0 liter/min) at the individual camera level. Currently we are working with the observatory to specify a two stage cooling system with liquid-liquid heat exchanger within the pier/tunnel underneath the telescope.

3. NOTABLE DESIGN ELEMENTS

In this section we collected some noteworthy features specific to the LLAMAS architecture. Some of these are discussed above or in the companion optics optics paper, including:

- gravity invariant mounting on telescope, near the telescope port – eliminating the need for flexure compensation and allowing for a high throughput, short fiber run;
- welded aluminum spectrograph unit frames that bolt together to form the Spectrograph Bay but serve as handling carts for the smaller sub-units – simplifying handling and shipping;
- mirrored symmetry in loading the vertically oriented, two-point mounted carbon fiber optical bench – resulting a very compact volume, providing a low thermal expansion, stiff reference for the optics and insensitive against potential stress in the support frame
- use of a dual side microlens array, paired with a passively aligned fiber plugplate – enabling maximal fill factor and high efficiency for the IFU;
- very fast refractive cameras designed with front and rear aspheres, larger elements in the middle of the optical train – accommodating the external pupil and the long slit.

Other aspects of the design philosophy not included in the System Architecture discussion are outlined in the sections below.

3.1 Economy of Scale

LLAMAS' science requirements (i.e. on information content per exposure) directly flow down into a minimum number of detector pixels needed by the instrument, but once that is set there are different strategies for illuminating the sensors. At one end of the spectrum, one could build one (or a few) large, mosaic detectors, coupled to a small number of similarly large optical elements with a single, long slit. The opposite extreme is to design around small format sensors and build compact, highly replicated systems with dozens of copies. The monolithic solution converges on a reflecting camera design, where central obscuration of the detector head can be significant. The multiplexed approach typically uses refractive cameras; because spectrographs need not correct lateral or axial color the lens train is manageable. From the very beginning we leaned toward the multiple smaller unit approach, but the big question was: where is the optimum?

For the LLAMAS design the number of pixels required in the dispersion direction is ∼6k, driven by the resolution, sampling and wavelength coverage. Thus we could have chosen a 6k format detector and a tall slit of ∼800 fibers and built only 3 spectrographs with a single optical arm in each. But this would have required glasses, AR coatings, optical designs, grating and detector efficiencies to be optimized over the entire 350-975nm passband. Using commoditized 1-2k format detectors results in more spectrographs but also smaller optical elements in a larger number of optical arms. However, this allows for passband optimized components. Three optical arms seemed sufficient to exploit such efficiency gain potentials, and choosing a $2k \times 2k$ CCD format we settled on the slit height of 300 fibers and thus 8 spectrographs.

We also considered elongated full frame $2k \times 1k$ formats or frame transfer devices with similar active area, but that would have doubled the number of spectrographs. Also, for COTS components it is hard to gain by ordering more units as being an established product the non recurring engineering (NRE) costs are already spread over many more units and customers. We needed some customization (bi-directional parallel clocking to enable nod & shuffle operation) so we had to buy enough units to bring the associated NRE share per unit to an acceptable/optimal level.

The situation is a bit different for the optical components. Those are completely custom (most of the time), and so setup-, tooling- and quality control (manufacturing tolerance) costs are unique to any given order. Therefore there is a significant cost saving potential by ordering larger number of components. We have somewhat limited test capabilities in our lab (see Sec. 4) and also considered the labor costs of the AIT phase when running our tolerance analysis. As a result we ended up prescribing more stringent requirements on optical fabrication

so as to loosen alignment criteria. This made the optics a bit pricier and incentivized batch production more. As an example: ordering the two prototype camera lens sets cost us 15% of the production of 27 units did for the final instrument. In other words the per unit costs dropped to half of what it was for the prototype.

But as mentioned there is also a cost in the assembly, integration and testing of the spectrographs as we now have eight of them to build. We tried to balance the costs of the increased and lengthened AIT phase by ordering tightly toleranced components. These increased the cost of manufacturing but simplified the assembly as we did not need to check components upon receipt, we could use smaller number of fixtures and subassemblies come together faster requiring less testing to meet specifications. Thus AIT costs dropped, and this seemed to be a win overall.

3.2 Carbon Fiber Optical Bench with Precision Inserts

As the spectrographs are mounted on the telescope we needed to athermalize the design. Weight was also a concern so we quickly moved away from conventional optical benches (with steel or invar faceplate) and converged towards a carbon fiber reinforced polymer (CFRP) structure.

The concept is to take advantage of the very low in-plane thermal expansion of the CFRP facesheet of the bench while using easily machined and cheap aluminum mounts for the optics and subassemblies. Since there is a large CTE mismatch between such mounts and the bench this requires anchoring the optical components in a particular way. We pick a point for each mount where a precision steel tooling ball is attached. This ball is then received by a precision steel bore embedded in the carbon fiber face sheet and fixes lateral positioning. (The height can be still adjusted as the ball can slide up and down in the cylinder.) Typically the location of these fixed reference points coincides with the vertex of the (front) optical element projected to the bench, which lays on the optical axis. The orientation of the mount is then set by another tooling ball, placed also in line with the local optical axis but as far away from the fixed vertex projection as possible. This second ball inserts into a precision slot of the bench. The remaining three degrees of freedom are set and locked by three push-pull adjuster screw pairs, located in a wide triangle on the mount base and contacting the bench at locations of embedded flat steel inserts. The preload applied by these is sufficient to keep the component in place, but lateral slip at the the bolted joints and the secondary ball sliding in its slot allows the base of the mount to "breathe" with respect to the CFRP face plate.

The prototype bench and such inserts can be seen on the left of Fig. 9. This used an aluminum honeycomb structure but for the production units the vendor suggested an internal CFRP rib structure to meet our stiffness requirements (see right side of figure). The lowest natural frequency of this bench is at 74Hz, while the maximum deflection under load expected to be less than 0.03mm. The symmetric load on the other side by the 2nd spectrograph also helps, but not just by canceling/balancing the load and having the load path stay inside the bench. Due to the mirrored symmetry in our architecture each insert has a counterpart at the exact same location on the opposite face. Therefore these inserts are not just embedded in the facesheets but also connected through bonded CFRP rods, which greately increases the stiffness. The precision inserts can be placed within 0.05mm, simplifying the integration process.

In the commercial space industry there are many vendors offering custom CFRP components. We found very wide variations (factor of 20) in quoted prices for the same components, and eventually selected CarbonVision from Germany, who offered the most competitive price for a given feature set. Working together on the prototype bench development we gained insight into their process that informed the design of benches for the facility instrument. Understanding the trades and costs better through prototyping the four production units we ordered have many additional, non-structural inserts on a regular grid pattern. These serve as cable tie-down points and attachment locations for baffles. We also specified a circular bolt pattern referenced directly into the bench, for attachment of the CMM arm (see Sec 3.4 used to align subassemblies during AIT.

3.3 Split Dichroich: Another Way to Embed Fibers

Although it was developed independently, the LLAMAS layout converged on many common design elements with the DESI spectrographs [4]. Its fiber pseudo-slit, which fans out to meet the Schmidt condition, must sit inside the collimated beam at the focus of the spherical collimator mirror. The first dichroic of the system must be placed at the slit. Behind it there is no room since the fibers need to be routed away and the second dichroic

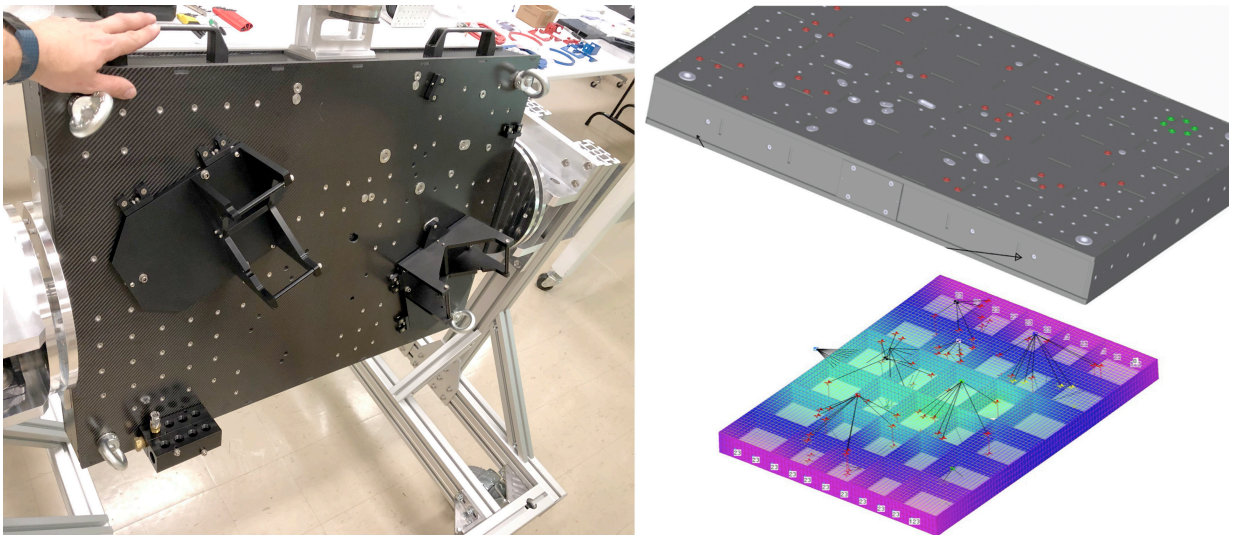

Figure 9.
The protoLLAMAS optical bench (left) on its handling cart, with the two camera cradles attached. This earleir bench design had an aluminum honeycomb structure, but the full instrument will have an internal carbon-fiber rib structure (see FE model, bottom right) for increased rigidity. We also requested more, regularly spaced general inserts besides the custom precision ones (top right) for easier cable management and attaching baffles. The green colored bolt pattern is to attach the CMM arm used for alignment.

also needs accommodation. The DESI dichroic features a tall open slot in the middle of it that allows feeding through the fiber slit. This has the advantage of a monolithic substrate and so the highly multi-layer coating can be deposited onto a continuous surface. However, getting a good coating to the edge of the slit opening without distortion and degradation of performance is still a challenge, as is machining the very narrow, angled slot into the substrate. This approach also requires the fibers to be mounted on a cantilevered slit plate, which is carefully fed through the dichroic aperture and independently supported/aligned.

We opted for a different design that placed tougher requirements on the dichroic manufacturing but simplifies AIT. If the dichroic is split in two halves then the slit plate can be bonded to the edge of one half, becoming part of the dichroic and not requiring its own support. The difficult machining operation of the angled slot is replaced with a simple "pocket cutting" operation at the angled edge of the split substrate. The edge of the substrate needs to be cut very clean and the coating has to go all the way to that the edge, without distorting the substrate, but that is also true for the DESI design (although the to-the-edge-coating is shorter there). In return we have a simple mounting scheme and full access to the slit, and comfortably can lay in the fibers. Another advantage that we only have one element to align – although the slit has to be precisely registered to the dichroic for the bonding. Finally, this assembly is fully athermal because fused silica is used for all elements: the dichroic substrate, the slit plate and the fibers.

With the split dichroic approach, mechanical obscuration from the pseudo-slit plate is small, under 2.5mm (see Fig 10). There is a thin, overall gap (< 0.5mm in our case), extending the full height of the dichroic. But the support blade that leads the fibers out of the collimated beam already obscures that thin vertical line. By making the pocket for the 1.5mm thick slit plate 2.0mm deep the fibers are recessed from the dichroic edge and are always protected, even if this 0.5mm gap fully closed.

Of course the challenge is to coat thin (10mm), tall (175mm) substrates all the way to the edge without chipping and distorting the glass. Another challenge is that the two sides have to be aligned parallel with sufficient precision ($< 1\lambda$), though we achieved this using 100 TPI adjusters. The adjusters required carbide inserts under the ball-end points to prevent creep, and ensure that the preloading bolts fell well within the support points. With these precautions bringing the two dichroic plates parallel was rapid using the 4 inch beam of a Zygo interferometer. Final alignment of the dichroic was performed using the spectrograph itself,

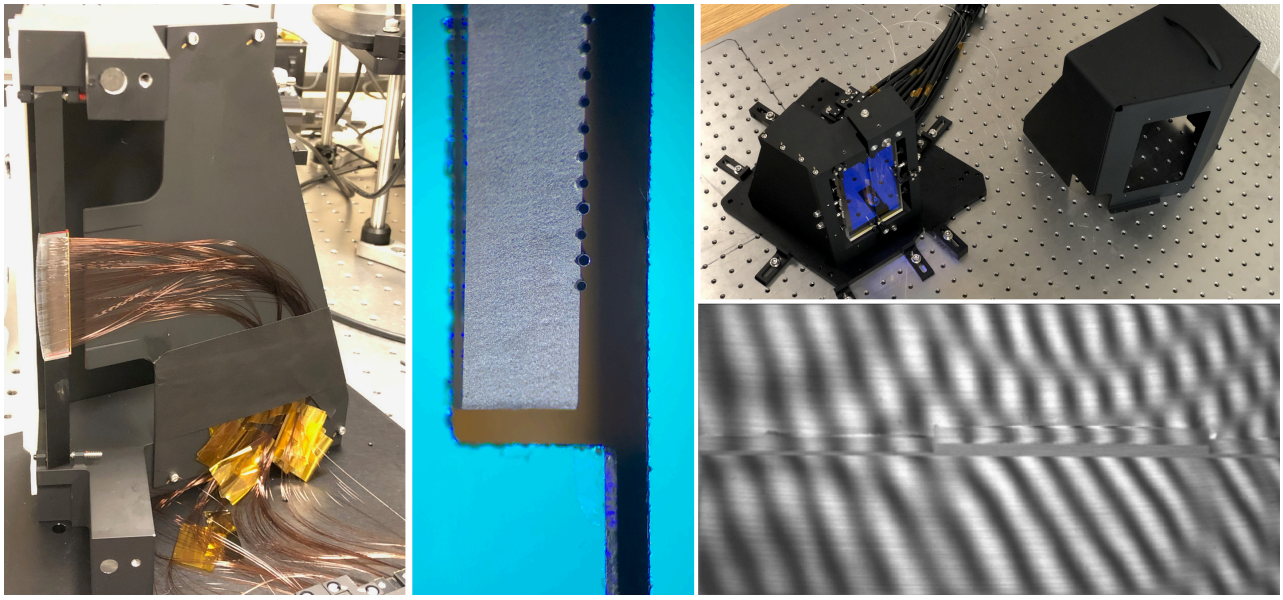

Figure 10.
Left: The stationary half of the dichroic, with the slit plate bonded and populated with fibers that lead away protected and strain relieved by the fiber blade. *Middle:* microscopic view of the assembled dichroic showing the corner of the slit plate, face on with the fibers. The slit plate is 1.5mm thick for reference. *Right:* the assembled dichroic with its cover removed, set up for interferometric testing (top) and the interferogram of the aligned halves (bottom, rotated view – the shadow of the slit plate is visible horizontally here). This shows a PV=0.96λ flatness across the two sides, with slight torsion of the lower part.

by comparing line centroids of emission features while alternating illumination between the two dichroic halves using a pupil mask.

We reached out to multiple vendors and selected Asahi Spectra Co. who met all specifications both for the split dichroics, and the monolithic blue/green dichroics as well. With Asahi's success at coating to the aperture edge, we prescribed a similar coating for the second dichroic to utilize a C-frame mount, making the optical layout even more compact.

3.4 Real-time Adjustment via Flex Bezels and use of a CMM

Given the large number of cameras to assemble we made a number of design choices that traded increased mechanical complexity for simpler, faster alignment. One such choice was to employ externally adjustable mounting bezels for strategically chosen lens elements. These allow for real time lateral adjustments that can be performed while the assembled camera is under optical testing. We also made the outer surface of these bezels not cylindrical but spherical, and mounted them to the optical train using fine threaded adjustable standoffs and coarse thread preloading screw pairs. This allows for axial (spacing) adjustment as well as tip-tilt corrections in a precision-fit barrel, without losing centration.

The most efficient compensators in the camera lens system are the two aspheres, which are the front and rear surfaces. Therefore for the prototype we mounted these elements in these flex bezels. Shown on the left panel of Fig 11 is the rear element of the prototype blue camera as its initial centration is set on an air bearing table using digital indicators. This was done right before optical centration against the other elements is verified/adjusted optically using a Trioptics OptiCentric collimator. The lateral flexures are independent, adjusted by two 100 TPI screws 90°apart (accessible through a hole on the barrel) that push against nylon tip spring preloaded plungers on the opposite sides. The tip-tilt and axial adjusting screw pairs are also visible.

Further analysis of the optical system and the final tolerance study showed we can fix the rear lens element so the production LLAMAS cameras only use one of these flex bezels holding the front lens element. To save

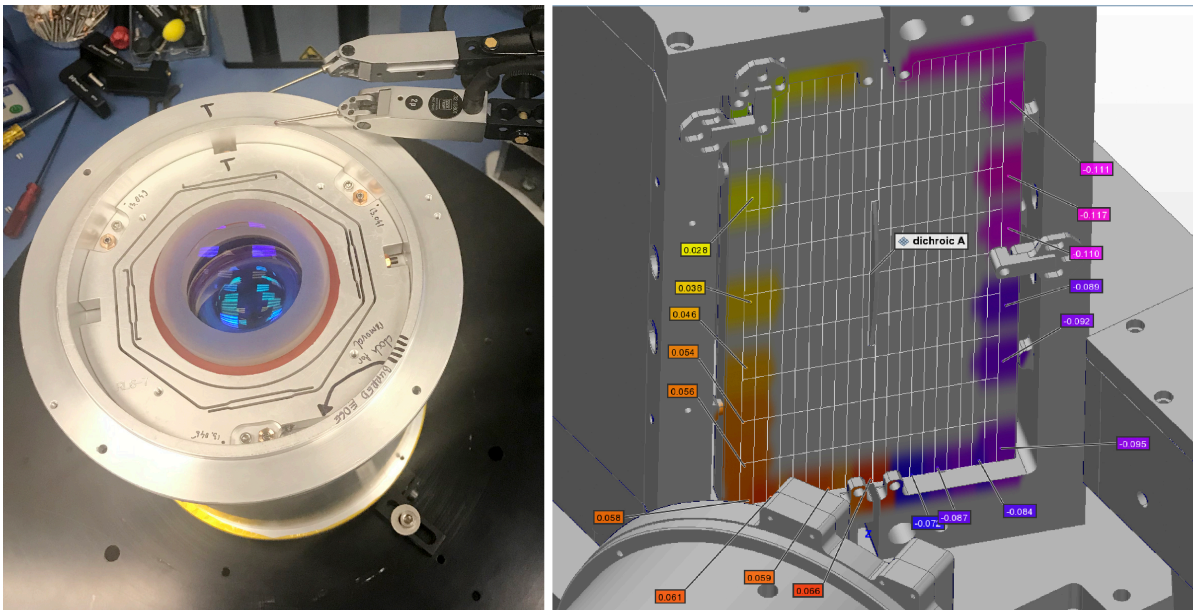

Figure 11.
Left: the flexure lens bezel allows for quick, real time centering adjustment. We also made the outer edge of the bezel spherical, with tight tolerance, so tip-tilt and spacing can be adjusted using push-pull actuators without loosing centration. *Right:* leaving an uncoated strip along the edge of the dichroic substrate and using a custom geometry CMM probe we could directly measure the position of the optics and map it directly into the CAD model.

cost, these elements are stacked for cutting on a single wire EDM setup. Therefore adding this feature, even prescribing the spherical outer facet and accounting for the extra hardware, only increased the price of each bezel by a few hundred dollars. For the prototype this flexibility saved significant time and personnel cost during AIT.

Another "real-time" alignment strategy involved direct measurement of reference element positions using a Hexagon coordinate measuring machine (CMM) arm. By prescribing generous clear apertures and using a custom, 60°bent, 140mm long, sapphire tipped probe we were able to map the location of the dichroic, the collimator, the grism, lens barrel and CCD camera positions directly onto the perfectly aligned CAD model of the instrument. An example is shown on the right panel Fig. 11 where the two halves of the split dichroic are probed at multiple locations, displaying the displacement from the ideal position as a heat map with numerical values. It is immediately apparent that the entire dichroic base is tiled along a horizontal axis with the top of the assembly tipped farther back in this view, by about $40\mu m$ compared to the bottom edge. There is no tilt along the vertical axis, and the left side of the dichroic is just 0.06mm away from its nominal position. What is also apparent, showcasing how good the CMM is (claimed precision of 0.02mm), that the right side of the split dichroic is somewhat offset, not co-planar with the fixed left side.

4. LESSONS LEARNED

In this section we summarize some of the lessons from the development of ProtoLLAMAS and LLAMAS that may apply to other highly multiplexed instruments.

System Complexity can manifest at design, integration, shipping, or commissioning

Aiming to lower system complexity is a good practice, but one can miss the point in the process as defining complexity can be ambiguous. A more complex part design might allow for simplified integration and/or operation, decreasing overall system complexity. So can happen the opposite. As an example: we originally we planned to employ one stepper motor to drive the focus for each detector head, as this would require "only" 24 focus motors (8 spectrographs × 3 channels) rather than the 72 needed to further control tip and tilt. The

motors would turn triplets of fine-pitch focus screws coupled via a timing belt. But for reliable operation a tight angular engagement of the belt is needed which required installation of multiple additional rollers/followers. In prototyping we found this assembly highly complex, time consuming to assemble, and hard to implement in a tight space.

Therefore we decided to directly drive each of the three actuators independently. Interestingly, the overall cost of this approach was still lower, even accounting for 3-fold increase in steppers and reduction gears (for necessary torque and resolution). The downside is a larger number of active components, and increased number of Arduino drivers needed, along with spares inventory and a bit more complex operation. However, these are offset by a major advantage discovered during AIT: the ability to remotely control tip-tilt, not just adjust the focus. If not for remote actuation each time tip-tilt adjustment was needed someone would have needed to go into the darkened clean room, remove instrument covers, make adjustments, reinstall the covers, and iterate. It was much more efficient adjusting the two cameras of the prototype with the three motors, and so it would be a significant time saving for the 24 cameras of the full instrument.

Trades: Fabrication benefits from economies of scale, Integration & Test do not

Building complexity into parts—whether optical elements, or opto-mechanical assemblies—may increase its manufacturing cost, but careful consideration of precision reference features often saved significant time during AIT, especially for highly replicated features. Once parts were designed and fixtured for machining we did achieve economies of scale for some custom fabrication elements, but the cost advantage from speeding integration and test was even more significant, since this is a serial job for the MIT research group.

Still, some machining jobs scale more favorably than others after considering tooling charges and other factors, so trades are never universal, and have to be judged on a case by case basis.

Prototyping

Especially for replicated systems, prototyping is a key strategy for reduction of technical and cost risk, and for LLAMAS our prototyping effort critically informed strategies for the facility instrument. We could evaluate not just design elements but also learn about new manufacturing processes, develop and exercise vendor relationships (minimizing procurement risk for the larger build), identify tooling needed for AIT, and time critical procedures.

For example, high order aspheres were until recently considered exotic or expensive. Today, aspheres on small optics (especially the benign ones LLAMAS employs) only marginally add to cost but they can dramatically improve image quality. Other interesting trades can appear for much simpler parts, such as a smooth cap with an rounded edge aperture on our flexible steel fiber hose that is critical to protect the fibers from being cut by the burred termination of the hose. We had $\sim$ 20 of these parts conventionally machined on a lathe for the prototype, but need nearly 400 of them for the full instrument. We will 3D these parts at 1% of the conventional machining costs while still meeting functionality requirements.

Additive manufacturing turned out to be an important cost-saving strategy for certain parts of the prototype. However we only explored which parts were appropriate for this method *after* the fact and not part of the original design process. This is less desirable as one could arrive potentially more optimal design solutions considering novel/alternate manufacturing processes during the initial design phase.

Maintaining vendor relationships with a long view

Vendors for astronomical instrumentation are often important, as some components have few sources, and our orders mean only modest profit margins for these companies compared to defense work. We benefit from their willingness to work with the scientific community, and maintaining those relationships can be important even during bumps in the road. During the LLAMAS prototype we encountered serious problems with one key vendor's quality control process. In response to exceptions we raised, they executed a full internal investigation, identified the root cause, and offered solutions moving forward. We agreed to contract with them for the facility instrument, but in a staged process to verify QC at critical steps. The vendor executed this next order with stellar performance, fixing everything that went wrong before, delivering on spec and ahead of schedule—directly in the heart of the COVID19 pandemic. The effort to work through initial challenges resulted in quite significant cost and schedule savings.

Metrology tool investments can be cost-effective in replicated instruments

The total value of a metrology tool is not measured by the price of purchase; one must also consider the cost to maintain expertise in its use by the team, but also the amount of time it will save during integration and test. We explored this trade for our CMM arm by a two stage approach. First, we rented a unit for the AIT phase of protoLLAMAS. While the learning curve was steep this experience was extremely valuable in identifying gross initial misalignment of a mechanical reference that would have been very difficult to identify optically. Following that experience we purchased a unit and invested in on-site training for our team.

Similarly we purchased a Trioptics OptiSurf long coherence length interferometer after observing that precision probing of lens vertex positions was important for the TESS, which had a similarly fast camera. It allows rapid, non-contact, precise (few μm) measurements of as-built element locations after all assembly tolerance stack-up. This allowed us to design the LLAMAS cameras with simple, cheap lens spacers with confidence that we can quickly measure and adjust spacers to achieve proper performance. This generates savings by reducing some of the machining tolerances and shortening testing, offsetting the initial investment in the metrology tool.

Alignment/tolerance simulations with sequenced compensator adjustment can speed integration

The Zemax simulations described above, where precision tolerances are flowed to the optics vendor, and alignment steps are followed in a precise order as compensators are adjusted, creates a deterministic plan for the last stages of AIT. The first light images from protoLLAMAS (Figure 12) were obtained after only adjusting the detector mounts for tilt and focus. Up to that point, the manufactured subsystems were assembled, installed in their mounts, placed on the optical bench, and adjusted using CMM feedback, at which point the system performed as designed.

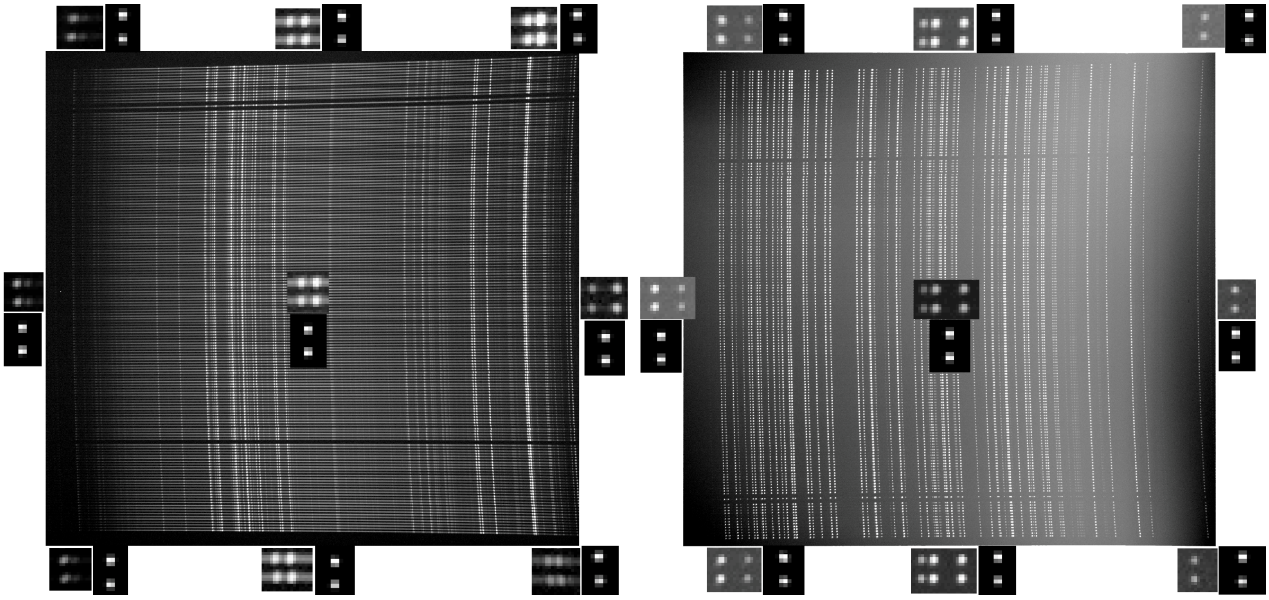

Figure 12.
With proper tolerance analysis, meeting the allowances in manufacturing and assembly as shown by component and subassembly level tests, and utilizing a CMM in the final integration step the image quality requirement was pretty much met out of the box. Left seen the blue, right on the red camera images from the prototype. Inserts provide zoomed in views in the corresponding locations. The black background insert are Zemax simulations of an ideally aligned camera, the gray background ones are the actual images. The background is diluted by stray light as this was truly a first light image with only a temporary cardboard enclosure over the instrument.

5. SUMMARY

We have successfully completed the build of the protoLLAMAS instrument and delivered it to Las Campanas Observatory in the spring of 2020. This prototype development provided key verification and refinement, along with technological risk reduction, for the full LLAMAS instrument build. This has been underway since early 2020, with all long lead items procured (some already delivered) and production of the replicated smaller subsystem components also nearing completion. At the writing of this article we have started the assembly and integration of components of the production unit spectrographs. Such AIT work is very challenging with the restrictions dictated by the ongoing pandemic, and there are undeniable impacts of global supply chain and manufacturing issues that materialize in our schedule and budget. Even during scaled-back laboratory activities we continue to make progress, though this sometimes required unconventional solutions like implementing makeshift laboratory stations at the homes of some team members. Accounting for these schedule perturbations, we project first light for LLAMAS at Magellan to happen in 2022.

Acknowledgments

Primary support for the construction of LLAMAS is provide by the National Science Foundation, under NSF MSIP grant 1836002. Funding for the development of protoLLAMAS came from the MIT Kavli Institute and Department of Physics.

REFERENCES

[1] The MUSE second-generation VLT instrument; Bacon et al, 2010, Proceedings of the SPIE, Volume 7735, id. 773508

[2] Commissioning and performances of the VLT-VIMOS instrument; Le Fèvre et al, 2003, Proceedings of the SPIE, Volume 4841, pp. 1670-1681

[3] WISDOM: the WIYN spectrograph for Doppler monitoring: a NASA-NSF concept for an extreme precision radial velocity instrument in support of TESS; Furesz et al, 2016, SPIE Proceedings Volume 9908, Ground-based and Airborne Instrumentation for Astronomy VI; 990814

[4] The DESI spectrograph system and production; Edelstein et al, 2018, Proc. SPIE 10702, Ground-based and Airborne Instrumentation for Astronomy VII, 107027G